



# VIBRATION STUDIES OF CROSS-PLY LAMINATED SHEAR DEFORMABLE CIRCULAR CYLINDERS ON THE BASIS OF ORTHOGONAL POLYNOMIALS

K. P. SOLDATOS

*Department of Theoretical Mechanics, University of Nottingham,  
Nottingham NG7 2RD, England*

AND

A. MESSINA

*Dipartimento di Scienza dei Materiali, Università di Lecce, 73100 Lecce, Italy*

*(Received 26 September 1997, and in final form 18 May 1998)*

This paper deals with a study of the free vibration characteristics of transverse shear deformable cross-ply laminated circular cylindrical shells on the basis of the Ritz method. The analysis is based on the energy functional of the Love-type version of the unified shell theory presented in reference [28]. As a result, several kinds of shear deformable Love-type shell theories are employed along with their classical counterpart. The theoretical formulation is given in a general form but the variational approach is finally applied in conjunction with a complete functional basis made of the appropriate admissible orthogonal polynomials. The method is currently capable of treating cross-ply laminated circular cylindrical shells subjected to any set of variationally consistent edge boundary conditions. In this paper, particular emphasis is given to the free vibrations of shells having one or both of their edges free of external tractions. The efficiency of the proposed method is exhibited by comparing corresponding results with certain experimental data, as well as with the very few existing relevant analytical results obtained elsewhere, on the basis of an alternative mathematical method (the state space concept). Apart the specific value of the present dynamic investigation, the analysis is further considered as a successful test towards its extension for the study of corresponding problems in which the state space concept cannot be applied directly.

© 1998 Academic Press

## 1. INTRODUCTION

The free vibrations of homogeneous orthotropic and cross-ply laminated complete circular cylindrical shells have been studied, to a considerable extent, on the basis of either classical or shear deformable shell theories. It is therefore well known that the state space concept [1–6] can provide an analytical solution to such a

vibration problem, for any set of boundary conditions imposed on the two shell edges. This is an exact method of solution and, regardless of the shell theory employed, it can further be applied for the free vibration study of complete cylindrical shells having arbitrary angle-ply lay-ups [6]. Although, in certain cases, its straightforward application may cause numerical instabilities, there are already available certain modified versions of the method [4, 7, 8] that can avoid such an ill-conditional behaviour.

The state space concept is essentially an exact analytical method for solving systems of simultaneous ordinary differential equations with constant coefficients. As far as the free vibration of cylindrical shells is concerned, it can therefore be applied to problems dealing with (i) complete circular cylinders, and (ii) open cylindrical panels having a rectangular plan-form and two opposite edges simply supported (a plate is an open cylindrical shell with zero curvature). In these cases, a suitable trigonometric choice of the displacement components can eliminate the dependency of the governing partial differential equations of motion from one of the two spatial co-ordinate parameters. Hence, it essentially converts these equations into ordinary differential equations with constant coefficients. When however vibrations of an open cylindrical panel (or a flat plate) with more complicated edge boundaries are investigated, the state space concept cannot be applied directly and therefore different analytical methods should be sought.

The method of expanding the unknown solution in an infinite series of certain basis functions (e.g., beam functions, polynomials) occurs then as a possible alternative mathematical approach. Provided that the set of basis functions is complete in the space of the functions that satisfy the edge boundary conditions assumed, the main task that remains is then to determine the unknown constant coefficients of such an infinite series. This may be achieved by using either a variational approach (e.g., the Ritz method) or an equivalent error minimisation technique (e.g., Galerkin's or modified Galerkin's method) [9]. Sometimes, such an infinite series solution is considered and treated as an approximate one. This however is mainly due to the fact that, in numerical applications, an infinite series has to be truncated to a certain finite number of terms. If an appropriately large number of terms is retained in that series, the exact solution to the problem can practically be achieved to any desired degree of accuracy. It should be noted, on the other hand, that an inappropriate basis may yield a very slowly converging series solution or to cause severe numerical instabilities. Hence, the choice of a "well behaving" set of basis functions is of particular importance.

The search of "well behaving" sets of basis functions, which are suitable for the dynamic analysis of homogeneous isotropic, orthotropic and composite laminated structural elements, has been a subject of investigation by itself. Its advances over the years have been recorded in several relevant publications and include the performance of beam characteristic functions [10–15], degenerated beam functions [13, 14], orthogonal characteristic polynomials [16–20] or even simple powers of the co-ordinate parameters [21–23]. Most of the work done in this subject is based on the application of the Ritz approach on the energy functional of classical plate and shell theories that ignore the effects of transverse deformation. These later

effects have been recognised as being of particular importance in the dynamic analysis of composite structures. Refined transverse deformable theories however have been employed only in a couple of relevant studies [18, 21], both of which dealt with vibrations of rectangular plates.

Many different combinations of edge boundary conditions have already been employed and studied in the references given above. There exists however a particular interest in the dynamic investigation of structural elements having some or all of their edges free of external tractions (see, for instance, references [1–4, 10–18, 24–26]). This is merely due to the fact that free edge boundaries are very common in engineering applications and relatively easy to achieve in a laboratory [25, 26]. Moreover, in the early stages of the aforementioned infinite series investigations, the accuracy of the predicted frequencies was significantly diminishing for plates having one or more of their edges free of tractions [10, 15, 27]. It should be noted however that more recent studies [16–18] have shown an excellent performance of the method, if appropriate orthogonal polynomials are chosen to form the basis of admissible functions.

This paper deals with a study of the free vibration characteristics of transverse shear deformable cross-ply laminated circular cylindrical shells on the basis of the Ritz method. The choice of the method is dictated from the intention to extend it, in due course, towards the study of corresponding problems in which the state space concept cannot be applied directly (e.g., statics and dynamics of shear deformable plates and open shells). In this respect, apart the specific value of the dynamic investigation presented in this paper, the analysis may be further considered as test study of the efficiency of the method in dealing with shear deformable laminated structures. The analysis is based on the energy functional of the Love-type version of the unified shell theory presented by Soldatos and Timarci [28] (see also references [5, 6]). As a result several kinds of shear deformable Love-type shell theories are employed along with their classical counterpart. The theoretical formulation is given in a general form but the variational approach is finally applied in conjunction with a complete functional basis made of the appropriate admissible orthogonal polynomials [16].

The method is capable of treating cross-ply laminated circular cylindrical shells subjected to any set of variationally consistent edge boundary conditions. In this paper, however, particular emphasis is given to the free vibrations of shells having one or both of their edges free of external tractions. In dealing with such example applications, more emphasis is given to the study of cross-ply laminated circular cylindrical shells, both edges of which are free of tractions. Under certain material restrictions, an experimental study of this problem was also performed and presented in a recent paper [26]. The problem, however, has not as yet been studied on the basis of an analytical approach and, therefore, relevant numerical results are not as yet available in the literature.

## 2. THEORETICAL FORMULATION

Consider a circular cylindrical panel, having a constant thickness  $h$  and an axial length  $L_x$  (Figure 1) and denote with  $R$  and  $L_s$  the radius and circumferential length

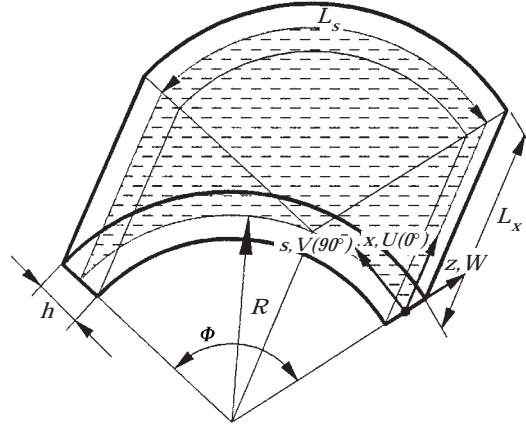


Figure 1. The nomenclature of a circular cylindrical panel.

of its middle-surface, respectively. For reasons that will become more evident later, it is theoretically advantageous to imagine the complete circular cylindrical shell considered as a particular case of this open panel for which  $\phi = 2\pi$ . Moreover, as the radius  $R$  approaches infinity ( $\phi = 0$ ), the geometrical configuration of a flat plate is obtained as another particular case. The axial, circumferential and normal to the middle-surface co-ordinate length parameters are denoted with  $x$ ,  $s$  and  $z$ , respectively, while  $U$ ,  $V$  and  $W$  represent the corresponding displacement components.

It is assumed further that the cylindrical panel considered is made of an arbitrary number,  $L$ , of linearly elastic orthotropic layers, the material axes of which coincide with the axes of the adopted curvilinear co-ordinate system. Hence, upon assuming negligible transverse normal stress and strain throughout the shell thickness, the stress-strain relationships in the  $k$ th layer (starting counting from the inner layer) are given as follows ( $k = 1, 2, \dots, L$ ):

$$\begin{bmatrix} \sigma_x^{(k)} \\ \sigma_s^{(k)} \\ \tau_{xs}^{(k)} \end{bmatrix} = \begin{bmatrix} Q_{11}^{(k)} & Q_{12}^{(k)} & 0 \\ Q_{12}^{(k)} & Q_{22}^{(k)} & 0 \\ 0 & 0 & Q_{66}^{(k)} \end{bmatrix} \begin{bmatrix} \varepsilon_x \\ \varepsilon_s \\ \gamma_{xs} \end{bmatrix}, \quad \begin{bmatrix} \tau_{sz}^{(k)} \\ \tau_{xz}^{(k)} \end{bmatrix} = \begin{bmatrix} Q_{44}^{(k)} & 0 \\ 0 & Q_{55}^{(k)} \end{bmatrix} \begin{bmatrix} \gamma_{sz} \\ \gamma_{xz} \end{bmatrix}, \quad (1)$$

where the appearing reduced stiffnesses are defined in reference [29].

The shell type approximations employed in this study are consistent with the general Love-type shear deformable shell theory detailed in references [5, 6, 28].

In this respect, only the main features and the basic equations of the theory are outlined in this section. These start with the general displacement approximation:

$$U(x, s, z; t) = u(x, s; t) - zw_{,x} + \Phi_1(z)u_1(x, s; t),$$

$$V(x, s, z; t) = (1 + z/R)v(x, s; t) - zw_{,s} + \Phi_2(z)v_1(x, s; t),$$

$$W(x, s, z; t) = w(x, s; t), \quad (2)$$

which then yields the following kinematic relations:

$$\varepsilon_x = u_{,x} - zw_{,xx} + \Phi_1(z)u_{1,x},$$

$$\varepsilon_s = (1 + z/R)v_{,s} - zw_{,ss} + \Phi_2(z)v_{1,s} + w/R,$$

$$\gamma_{sz} = \Phi_2'v_1,$$

$$\gamma_{xz} = \Phi_1'u_1,$$

$$\gamma_{xs} = u_{,s} + v_{,x} + z(-2w_{,xs} + v_{,x}/R) + \Phi_1u_{1,s} + \Phi_2v_{1,x}, \quad (3)$$

where a prime denotes differentiation with respect to  $z$ . Here,  $u$ ,  $v$ ,  $w$ ,  $u_1$  and  $v_1$  are the five unknown displacement functions (degrees of freedom) of the theory, while  $\Phi_1(z)$  and  $\Phi_2(z)$  represent the *a posteriori* specified shape functions which, through their derivatives, determine the through-the-thickness distribution of the transverse shear strains or stresses [5, 28].

The force and moment resultants of the theory are defined according to,

$$(N_x, N_s, N_{xs}) = \int_{-h/2}^{h/2} (\sigma_x, \sigma_s, \tau_{xs}) dz, \quad (M_x, M_s, M_{xs}) = \int_{-h/2}^{h/2} (\sigma_x, \sigma_s, \tau_{xs})z dz,$$

$$(M_x^a, M_{xs}^a) = \int_{-h/2}^{h/2} (\sigma_x, \tau_{xs})\Phi_1(z) dz, \quad (M_s^a, M_{sx}^a) = \int_{-h/2}^{h/2} (\sigma_s, \tau_{sx})\Phi_2(z) dz,$$

$$Q_x^a = \int_{-h/2}^{h/2} \tau_{xz}\Phi_1' dz, \quad Q_s^a = \int_{-h/2}^{h/2} \tau_{sz}\Phi_2' dz, \quad (4)$$

and, after equations (1), they yield the following constitutive equations:

$$\begin{bmatrix} N_x \\ N_s \\ N_{xs} \\ M_x \\ M_s \\ M_{xs} \\ M_x^a \\ M_s^a \\ M_{xs}^a \\ M_{sx}^a \end{bmatrix} = \begin{bmatrix} A_{11} & A_{12} & 0 & B_{11} & B_{12} & 0 & B_{111} & B_{122} & 0 & 0 \\ A_{12} & A_{22} & 0 & B_{12} & B_{22} & 0 & B_{121} & B_{222} & 0 & 0 \\ 0 & 0 & A_{66} & 0 & 0 & B_{66} & 0 & 0 & B_{661} & B_{662} \\ B_{11} & B_{12} & 0 & D_{11} & D_{12} & 0 & D_{111} & D_{122} & 0 & 0 \\ B_{12} & B_{22} & 0 & D_{12} & D_{22} & 0 & D_{121} & D_{222} & 0 & 0 \\ 0 & 0 & B_{66} & 0 & 0 & D_{66} & 0 & 0 & D_{661} & D_{662} \\ B_{111} & B_{121} & 0 & D_{111} & D_{121} & 0 & D_{1111} & D_{1212} & 0 & 0 \\ B_{122} & B_{222} & 0 & D_{122} & D_{222} & 0 & D_{1212} & D_{2222} & 0 & 0 \\ 0 & 0 & B_{661} & 0 & 0 & D_{661} & 0 & 0 & D_{6611} & D_{6612} \\ 0 & 0 & B_{662} & 0 & 0 & D_{662} & 0 & 0 & D_{6612} & D_{6622} \end{bmatrix} \begin{bmatrix} u_x \\ v_s + \frac{W}{R} \\ u_s + v_{,x} \\ -W_{,xx} \\ -W_{,ss} + \frac{v_s}{R} \\ -2W_{,xs} + \frac{v_x}{R} \\ u_{1,x} \\ v_{1,s} \\ u_{1,s} \\ v_{1,x} \end{bmatrix}, \tag{5}$$

$$\begin{bmatrix} Q_s^a \\ Q_x^a \end{bmatrix} = \begin{bmatrix} A_{4422} & 0 \\ 0 & A_{5511} \end{bmatrix} \begin{bmatrix} v_1 \\ u_1 \end{bmatrix}.$$

Here, the appearing rigidities are defined as follows:

$$\begin{aligned}
 A_{ij} &= \int_{-h/2}^{h/2} Q_{ij}^{(k)} dz, & A_{jll} &= \int_{-h/2}^{h/2} Q_{ij}^{(k)} (\Phi_l')^2 dz, \\
 B_{ij} &= \int_{-h/2}^{h/2} Q_{ij}^{(k)} z dz, & B_{ijl} &= \int_{-h/2}^{h/2} Q_{ij}^{(k)} \Phi_l dz, \\
 D_{ij} &= \int_{-h/2}^{h/2} Q_{ij}^{(k)} z^2 dz, & D_{ijl} &= \int_{-h/2}^{h/2} Q_{ij}^{(k)} \Phi_l z dz, & D_{ijlm} &= \int_{-h/2}^{h/2} Q_{ij}^{(k)} \Phi_l \Phi_m dz,
 \end{aligned}
 \tag{6}$$

with indices taking their appropriate values.

The variationally consistent equations of motion as well as the corresponding sets of edge boundary conditions are given, in terms of the afore mentioned quantities, in reference [28]. Here, however, the Ritz method will be used. In this respect, the five unknown displacement functions are expressed in the following form:

$$u(x, s; t) = \cos(\omega t) \sin(n\pi s/L_s) \sum_{m=1}^M A_m X_m^u(x),$$

$$v(x, s; t) = \cos(\omega t) \cos(n\pi s/L_s) \sum_{m=1}^M B_m X_m^v(x),$$

$$w(x, s; t) = \cos(\omega t) \sin(n\pi s/L_s) \sum_{m=1}^M C_m X_m^w(x),$$

$$u_1(x, s; t) = \cos(\omega t) \sin(n\pi s/L_s) \sum_{m=1}^M D_m X_m^{u_1}(x),$$

$$v_1(x, s; t) = \cos(\omega t) \cos(n\pi s/L_s) \sum_{m=1}^M E_m X_m^{v_1}(x), \tag{7}$$

where  $\omega$  is an unknown natural frequency of vibration. The  $s$ -dependent parts in these representations enable the satisfaction of simple support boundary conditions on the straight edges of an open panel ( $s = 0, L_s$ ) or, provided that the half-wave number  $n$  is an even integer, the satisfaction of all the periodicity requirements that should hold around the circumference of a closed cylindrical shell ( $\phi = 2\pi$ ).

Each of the summations appearing in equations (7) represents a series expansion of the unknown  $x$ -dependent part of the corresponding displacement function. The set of the appearing basis functions should be chosen to be complete in the space of the functions that satisfy the geometric boundary conditions employed at the curved shell edges ( $x = 0, L_x$ ). Each member of the basis functions is multiplied by an unknown constant coefficient, the whole set of which is to be determined on the basis of a variational method (e.g., the Ritz method). Under these considerations, such a variational method can, in principle, yield an exact series-form representation of the solution sought, provided that  $M = \infty$ . In practice, however, each of the series appearing in equations (7) should be truncated to a finite number of terms, which may differ from one expression to another. For simplicity, the same number of such terms,  $M$ , is assumed throughout this paper for all five series expansions.

The Ritz method requires the determination of the unknown coefficients appearing in equations (7) by minimizing the total Lagrangian of the system over a certain time interval. This is equivalent with applying Hamilton's principle:

$$\delta \int_{t_1}^{t_2} (T - \hat{U}) dt = 0, \quad (8)$$

where the appearing kinetic and the strain energies are given according to,

$$T = \frac{1}{2} \int_{Vol} \rho (\dot{U}^2 + \dot{V}^2 + \dot{W}^2) dz ds dx, \quad (9)$$

$$\hat{U} = \frac{1}{2} \int_{Vol} (\sigma_x \varepsilon_x + \sigma_s \varepsilon_s + \tau_{sz} \gamma_{sz} + \tau_{xz} \gamma_{xz} + \tau_{xs} \gamma_{xs}) dz ds dx.$$

Equation (8) is essentially equivalent with setting equal to zero all the  $5M$  partial derivatives of its integrand, with respect to the same number of the unknown coefficients appearing in equation (7). It therefore yields the following generalized algebraic eigenvalue problem:



$$\begin{aligned}
 & \left[ \begin{array}{c} [K] \\ [M] \end{array} \right] \cdot \left[ \begin{array}{c} \mathbf{A} \\ \mathbf{B} \\ \mathbf{C} \\ \mathbf{D} \\ \mathbf{E} \end{array} \right] = \mathbf{0}, \quad (10) \\
 & \int_0^{L,x} \left[ \begin{array}{c} \mathbf{k}_{11} \quad \mathbf{k}_{12} \quad \mathbf{k}_{13} \quad \mathbf{k}_{14} \quad \mathbf{k}_{15} \\ \mathbf{k}_{12}^T \quad \mathbf{k}_{22} \quad \mathbf{k}_{23} \quad \mathbf{k}_{24} \quad \mathbf{k}_{25} \\ \mathbf{k}_{13}^T \quad \mathbf{k}_{23}^T \quad \mathbf{k}_{33} \quad \mathbf{k}_{34} \quad \mathbf{k}_{35} \\ \mathbf{k}_{14}^T \quad \mathbf{k}_{24}^T \quad \mathbf{k}_{34}^T \quad \mathbf{k}_{44} \quad \mathbf{k}_{45} \\ \mathbf{k}_{15}^T \quad \mathbf{k}_{25}^T \quad \mathbf{k}_{35}^T \quad \mathbf{k}_{45}^T \quad \mathbf{k}_{55} \end{array} \right] - \omega^2 \int_0^{L,x} \left[ \begin{array}{c} \mathbf{m}_{11} \quad \mathbf{0} \quad \mathbf{0} \quad \mathbf{0} \quad \mathbf{0} \\ \mathbf{0} \quad \mathbf{m}_{22} \quad \mathbf{m}_{23} \quad \mathbf{0} \quad \mathbf{m}_{25} \\ \mathbf{0} \quad \mathbf{m}_{23}^T \quad \mathbf{m}_{33} \quad \mathbf{m}_{34} \quad \mathbf{m}_{35} \\ \mathbf{0} \quad \mathbf{0} \quad \mathbf{m}_{34}^T \quad \mathbf{m}_{44} \quad \mathbf{0} \\ \mathbf{0} \quad \mathbf{m}_{25}^T \quad \mathbf{m}_{35}^T \quad \mathbf{0} \quad \mathbf{m}_{55} \end{array} \right]
 \end{aligned}$$

where the appearing  $M \times M$  stiffness and inertia submatrices are given in Appendix A.

As has already been mentioned, the basis functions employed in this paper are orthogonal polynomials that satisfy all the geometric boundary conditions applied at the curved shell edges [16, 17]. In more detail, given the first of these polynomials,  $\psi_1(x)$ , the remaining ones are constructed according to the following recursive formulas [16]:

$$\begin{aligned}\psi_2(x) &= (x - B_2)\psi_1(x), \\ \psi_k(x) &= (x - B_k)\psi_{k-1}(x) - C_k\psi_{k-2}(x), \quad \text{for } k > 2, \\ B_k &= \frac{\int_0^{L_x} x\psi_{k-1}^2(x) dx}{\int_0^{L_x} \psi_{k-1}^2(x) dx}, \quad C_k = \frac{\int_0^{L_x} x\psi_{k-1}(x)\psi_{k-2}(x) dx}{\int_0^{L_x} \psi_{k-2}^2(x) dx}.\end{aligned}\quad (11)$$

Upon further dividing each one of its members by the square root of the norm:

$$\|\psi_k(x)\| = \int_0^L \psi_k^2(x) dx, \quad (12)$$

the orthogonal polynomial basis developed is converted into a corresponding orthonormal one.

As will be seen in the next section with a particular example, such an orthonormal basis behaves better than its orthogonal counterpart, in the sense that it improves considerably the numerical stability of the final algebraic eigenvalue problem (10). All numerical results presented in the next section are for open cylindrical panels and closed cylindrical shells having both their curved edges free of external tractions (FF shells) or one of these edges clamped and the other free of tractions (CF shells). Since there are no geometric boundary conditions applied on a free edge, all the orthonormal bases used for the numerical study of FF shells and panels start with the zeroth degree polynomial and, therefore,

$$X_1^u(x) = X_1^v(x) = X_1^w(x) = X_1^{u1}(x) = X_1^{v1}(x) = (L_x)^{-1/2}. \quad (13)$$

For CF shells, however, all displacement components must be zero at  $x = 0$  while, in addition, the first derivative of  $w$  must be zero at  $x = 0$ . Hence, the orthonormal bases used in this case are as follows:

$$\begin{aligned}X_1^u(x) &= X_1^v(x) = X_1^{u1}(x) = X_1^{v1}(x) = x(L_x^3/3)^{-1/2}, \\ X_1^w(x) &= x^2(L_x^5/5)^{-1/2}.\end{aligned}\quad (14)$$

The elements of the stiffness and mass matrices appearing in equation (10) become therefore products of polynomial functions and the denoted integrations can be carried out numerically, up to any desired degree of accuracy.

## 3. NUMERICAL EXAMPLES

As has already been mentioned, the emphasis in this section is on the vibration characteristics of cross-ply laminated circular cylindrical shells having one or both of their curved edges free of external tractions. For such shells, numerical results that are based on alternative mathematical methods are very rare in the literature. In order to check the reliability of the method presented in the preceding sections, some comparisons were initially performed with corresponding numerical results obtained by Khdeir *et al.* [3] on the basis of the state space concept. These are for open cylindrical panels having both their straight edges simply supported and their curved edges free of external tractions (SSFF panels). Each one of these panels is assumed to be made of a certain number of specially orthotropic layers, all of which have the following material properties:

$$E_1/E_2 = 25, \quad G_{12}/E_2 = G_{13}/E_2 = 0.5, \quad G_{23}/E_2 = 0.2, \quad \nu_{12} = 0.25. \quad (15)$$

Khdeir *et al.* [3] applied the state space concept on the equations of a parabolic shear deformable shell theory that is obtained by choosing the following form of the shape functions appearing in equations (2):

$$\Phi_1(z) = \Phi_2(z) = z(1 - 4z^2/3h^2). \quad (16)$$

This choice of the shape functions yields a through the thickness parabolic distribution of the transverse shear strains. After equations (1) and (3), it therefore guarantees the satisfaction of the zero shear traction boundary conditions imposed on the shell lateral surfaces, but it violates the continuity of interlaminar stresses at the shell material interfaces. Hence, in order to keep the line followed in reference [5], all results based on the choice (16) will be indicated with the notation PAR<sub>ds</sub> (parabolic shear deformation—discontinuous stresses). For comparison purposes, the shape functions (16) are initially used for the results shown in Tables 1–3.

For both the orthogonal and the orthonormal FF polynomial functional bases described in the preceding section, Table 1 shows the value of the fundamental frequency parameter,

$$\bar{\omega} = \frac{\omega L_x^2}{h} \sqrt{\rho/E_2}, \quad (17)$$

obtained upon increasing the number of the polynomial terms involved in expressions (7). These results make evident a fast convergence of the frequency parameter, towards the corresponding value obtained in reference [3] on the basis of the state space concept ( $\bar{\omega} = 5.7$ ). For either of the two functional bases, three terms in the series expansion (7) are adequate to provide the exact frequency with an accuracy of four significant figures. Moreover, the two frequency columns shown in Table 1 cannot reveal by themselves any differences or benefits in using any one of the two polynomial bases instead of the other. The two extra columns added for each basis, give however the condition number of the stiffness and the inertia matrix, respectively, that is the ratio of the largest to the smallest singular value of the matrix (see reference [30, p. 61]).

TABLE 1

*Convergence of the fundamental frequency parameter,  $\bar{\omega}$ , of an SSFF open  $[0^\circ/90^\circ]$  circular cylindrical panel ( $R/L_x = 5$ ,  $L_x/L_s = 1$ ,  $L_x/h = 10$ ,  $n = 1$ ;  $PAR_{ds}$ ). State space concept value [3]:  $\bar{\omega} = 5.7$*

$M$	Orthogonal polynomials			Orthonormal polynomials		
	$\bar{\omega}$	Cond( $K$ )	Cond( $M$ )	$\bar{\omega}$	Cond( $K$ )	Cond( $M$ )
1	5.744	7.80E + 02	1.88E + 03	5.744	7.80E + 02	1.88E + 03
2	5.742	8.90E + 03	2.26E + 04	5.742	9.53E + 02	1.92E + 03
3	5.741	1.10E + 05	3.39E + 05	5.741	4.64E + 03	2.07E + 03
4	5.741	1.43E + 06	5.27E + 06	5.741	1.31E + 04	2.45E + 03
5	5.741	1.83E + 07	8.31E + 07	5.741	2.94E + 04	3.24E + 03
6	5.741	2.35E + 08	1.32E + 09	5.741	5.79E + 04	4.85E + 03
7	5.741	3.06E + 09	2.09E + 10	5.741	1.06E + 05	8.03E + 03
8	5.741	4.08E + 10	3.33E + 11	5.741	2.01E + 05	1.42E + 04
9	5.741	5.58E + 11	5.31E + 12	5.741	4.30E + 05	2.58E + 04
10	5.741	7.79E + 12	8.46E + 13	5.741	8.82E + 05	4.69E + 04

The condition numbers have not the presumption of some general parameters that assess the behaviour of an orthogonal basis. They however provide useful information with regard to the eventual numerical treatment [30] of the stiffness and the inertia matrices that represent the generalized eigenvalue problem (10). In this respect, Table 1 makes clear that, if many terms are retained in the series expansion (7), the orthonormal polynomial basis behaves better than the orthogonal one, in the sense that it keeps the condition number of both matrices within reasonably low bounds. On the other hand, the convergence of the results presented in Table 1 is extremely fast and, therefore, the exact fundamental frequency parameter is obtained by retaining only the first few terms in the series expansions (7). There are cases however, particularly when higher vibration frequencies are sought, in which many terms should be retained in the series expansion (7). Since in such cases the condition number of the stiffness and the inertia matrices should be kept as low as possible, only the orthonormal bases will be used for the remaining results throughout this section. All the results presented in this section were obtained by employing numerical codes that made use of the standard mathematical functions of MATLAB V.4.2.

Under these considerations, Tables 2 and 3 present further SSFF open panel results that reveal several features of the behaviour of the present method. In more detail, Table 2 shows the complete comparison of all fundamental frequency parameters obtained in reference [3] on the basis of the state space concept, with the corresponding ones obtained on the basis of the present approach, for different numbers of polynomial terms. This comparison clarifies that, upon retaining only the first three polynomial terms in the series expansion (7), the present method always predicts the exact vibration frequency within accuracy of four significant figures. Table 3 finally shows the influence of the polynomial number  $M$  on the six first frequency parameters  $\bar{\omega}$  of the cylindrical panel that has already

TABLE 2

*Convergence of the fundamental frequency parameter,  $\bar{\omega}$ , of SSFF open circular cylindrical panels ( $L_x/L_s = 1$ ,  $L_x/h = 10$ ,  $n = 1$ ;  $PAR_{ds}$ )*

$M$	$[0^\circ/90^\circ/0^\circ]$		$[0^\circ/90^\circ]$	
	$R/L_x = 5$	$R/L_x = 20$	$R/L_x = 5$	$R/L_x = 20$
1	3.770	3.791	5.744	5.811
2	3.768	3.790	5.742	5.810
3	3.767	3.789	5.741	5.809
4	3.767	3.789	5.741	5.809
5	3.767	3.789	5.741	5.809
Reference [3]	3.783	3.789	5.7	5.8

been employed in Table 1. Moreover, Figure 2 shows a mapping, into the square domain  $[0, 1] \times [0, 1]$ , of the transverse component,  $w$ , of the part of the corresponding mode shapes that acts on the panel middle-surface ( $z = 0$ ).

Apart from the good practice of identifying vibration frequencies on the basis of their mode shape, the results shown in Table 3 and in Figure 2 enable the observation of some additional features of the convergence process. Upon considering the nature of the orthonormal polynomials generated with the recursive formulas (11) and (12), it becomes evident that a very accurate prediction of a frequency and the corresponding mode shape is achieved when the degree of the highest polynomial employed in expression (7) approaches or slightly exceeds the associated mode number. Figure 2(b), for instance, reveals that the mode shape of the second frequency can be built accurately by making use of, at most, first-degree polynomials. Moreover, at that stage, the predicted second frequency parameter has already approached as close as 1% to its final value obtained by

TABLE 3

*Convergence of the frequency parameter,  $\bar{\omega}$ , of an SSFF open  $[0^\circ/90^\circ]$  circular cylindrical panel for several values of the circumferential wave number,  $n$  ( $R/L_x = 5$ ,  $L_x/L_s = 1$ ,  $L_x/h = 10$ ;  $PAR_{ds}$ )*

$M$	Circumferential half-wave number $n$					
	1	2	3	4	5	6
1	5.744	—	—	—	—	—
2	5.742	6.942	—	—	—	—
3	5.741	6.941	18.242	21.828	—	—
4	5.741	6.902	17.654	20.992	44.368	—
5	5.741	6.901	15.905	20.971	40.993	77.800
6	5.741	6.879	15.842	20.773	33.050	72.080
7	5.741	6.879	15.773	20.773	32.713	54.112
8	5.741	6.872	15.772	20.756	32.351	53.351
9	5.741	6.872	15.765	20.756	32.342	51.895
10	5.741	6.870	15.765	20.754	32.340	51.851

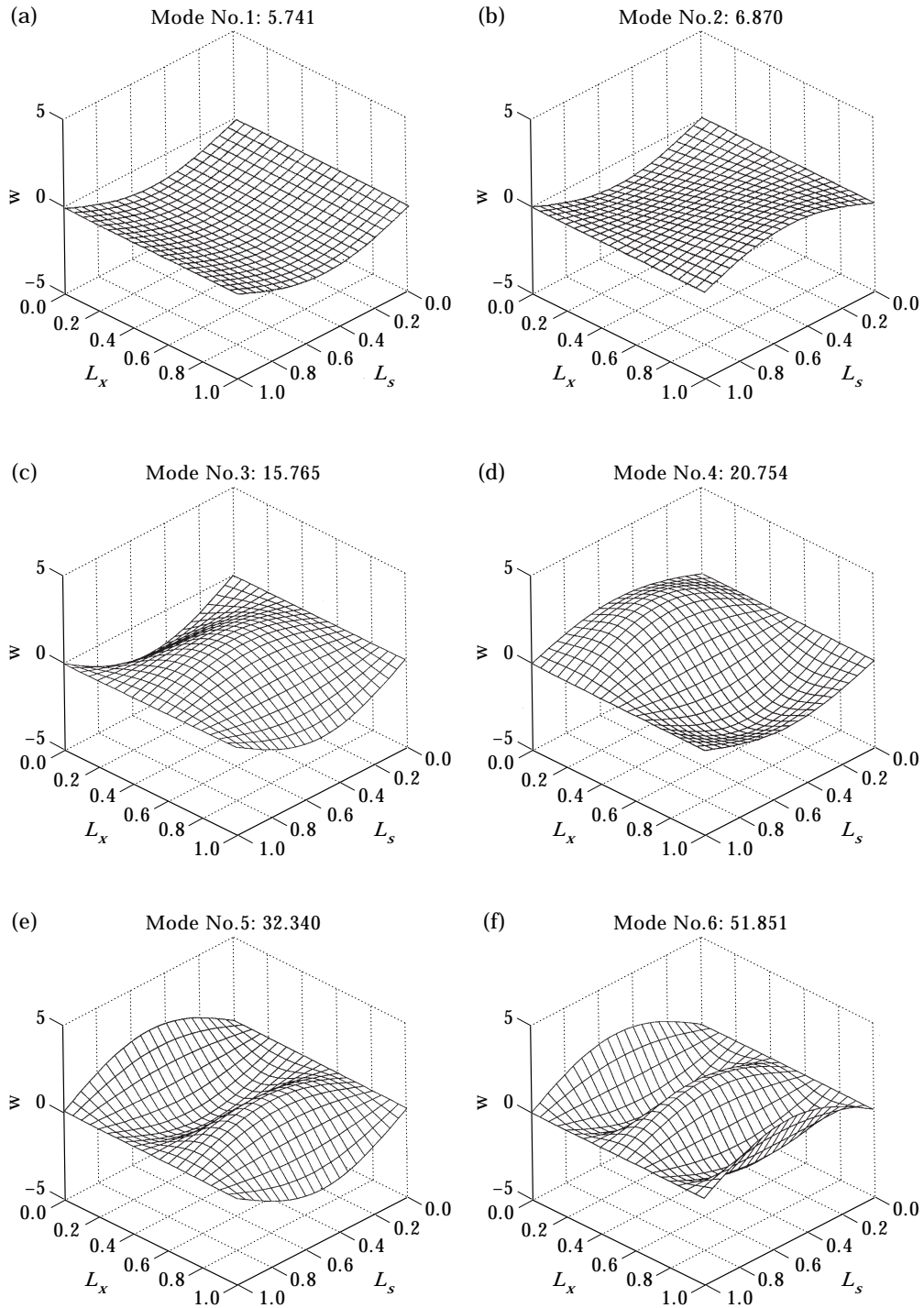


Figure 2. Transverse component of the mode shapes corresponding to the frequencies tabulated in Table 3.

retaining ten polynomial terms. Similarly, the mode shape of the sixth mode is built very accurately by employing the first eight or nine orthonormal polynomials. This complicated mode shape [Figure 2(f)] would however never be determined by superposing the first three orthonormal polynomials, which represent a constant (translation), a straight line (rotation) and a parabola. This later argument also makes evident the reason for the existence of the big gap between the prediction of the sixth frequency obtained by retaining the first five (77.80) and the first seven polynomial terms (54.112) in expression (7).

The influence of different types of shell theories, as well as the influence of the  $h/R$  and  $L_x/R$  ratios, on the fundamental frequencies of certain FF complete circular cylinders having a symmetric  $[0^\circ/90^\circ/0^\circ]$  lay-up, are shown in Tables 4 ( $h/R = 0.02$ ) and 5 ( $h/R = 0.2$ ). The results tabulated in these tables, as well as all numerical results shown in what follows, were found to be very accurate by employing  $M = 8$  in the polynomial expansions (7). For comparison purposes, the classical Love-type shell theory (CST), its uniform shear deformable analogue (UNI), as well as two versions of its parabolic shear deformable analogue were used for the results presented in Tables 4 and 5. In more detail, apart from the afore mentioned  $PAR_{ds}$  version of the shear deformable theory, its more advanced version that accounts for the through-thickness continuity of the parabolically distributed interlaminar stresses [5] was also employed. All results based on this advanced version of the theory are indicated with the notation  $PAR_{cs}$  (parabolic shear deformation—continuous stresses). In this version, the global shape functions  $\Phi_1(z)$  and  $\Phi_2(z)$  can be derived by applying the general iterative approach described in reference [5], after assuming three sets of local shape functions of the form (16) (one set of shape functions for each layer). In order to avoid any possible drawbacks of a slight approximation involved in the iterative approach proposed in reference [5], an alternative exact approach was also employed in this paper. This is briefly outlined in Appendix B for cylinders having a symmetric lay-up and, in its present form, holds only for the case that all sets of local shape functions involved have the form (16). It should be emphasized, however, that using either the previous iterative approach [5] or its present improvement, the advanced version of the shear deformable shell theory produced essentially identical results. Hence, only one set of such frequencies is always shown, under the notation  $PAR_{cs}$ .

TABLE 4

*Fundamental frequency parameters,  $\bar{\omega}$ , of an FF open  $[0^\circ/90^\circ/0^\circ]$  circular cylindrical shell ( $h/R = 0.02$ ,  $n = 4$ ,  $E_1 = 40E_2$ ,  $G_{12} = G_{13} = 0.6E_2$ ,  $G_{23} = 0.5E_2$ ,  $\nu_{12} = 0.25$ )*

Theory	$L_x/R$								
	0.20	0.25	0.5	0.75	1.00	1.25	1.50	1.75	2.00
CST	0.04846	0.07572	0.3029	0.6816	1.212	1.893	2.727	3.711	4.848
UNI	0.04845	0.07570	0.3028	0.6814	1.212	1.893	2.726	3.710	4.846
$PAR_{ds}$	0.04844	0.07569	0.3028	0.6813	1.211	1.893	2.726	3.710	4.845
$PAR_{cs}$	0.04844	0.07569	0.3028	0.6813	1.211	1.893	2.726	3.710	4.846

TABLE 5

*Fundamental frequency parameter,  $\bar{\omega}$ , of an FF closed  $[0^\circ/90^\circ/0^\circ]$  circular cylindrical shell ( $h/R = 0.02$ ,  $n = 4$ ,  $E_1 = 40E_2$ ,  $G_{12} = G_{13} = 0.6E_2$ ,  $G_{23} = 0.5E_2$ ,  $\nu_{12} = 0.25$ )*

Theory	$L_x/R$								
	0.20	0.25	0.5	0.75	1.00	1.25	1.50	1.75	2.00
CST	0.04828	0.07544	0.3018	0.6790	1.207	1.886	2.716	3.697	4.830
UNI	0.04689	0.07326	0.2931	0.6594	1.172	1.832	2.638	3.590	4.689
PAR <sub>ds</sub>	0.04628	0.07230	0.2892	0.6508	1.157	1.808	2.603	3.543	4.628
PAR <sub>cs</sub>	0.04645	0.07257	0.2903	0.6531	1.161	1.814	2.613	3.556	4.645

Both Tables 4 and 5 clarify that the parabolic shear deformable theories always give lower frequencies than their corresponding CST and UNI counterparts. For very thin shells (Table 4), this does not give a particular advantage to any of the theories compared. As was expected, all three theories yield practically identical fundamental frequencies and, therefore, even the CST is reliable. For thicker shells however (Table 5), the CST should be abandoned completely and its parabolic shear deformable analogue should be preferred. The fact that the PAR<sub>ds</sub> model underestimates in some cases while in other cases overestimates the frequency parameters obtained by the more accurate PAR<sub>cs</sub> model has also been reported in references [5, 6, 31, 32] and, therefore, it does not come as a surprise. It should be reasonable to expect, in this respect, that further progress of the corresponding solutions that are based on three-dimensional theory of elasticity (see, for instance, references [33–37]) will confirm the superiority of the PAR<sub>cs</sub> model.

The results presented in Tables 4 and 5 show further that, regardless of the shell theory employed, the length of such stiff cylinders has a very little effect on their circular fundamental frequency parameter,  $\omega$  (rad/s). This can easily be verified upon dividing all the  $\bar{\omega}$ s tabulated in these tables by their corresponding  $L_x^2$  values and, then, by comparing all these outputs obtained for the same shell theory. It means that, for so stiff FF cylinders ( $E_1/E_2 = 40$ ), the fundamental circular frequencies are principally influenced by bending effects and only very slightly by corresponding in-plane shear deformations. Hence, the dynamic behaviour of such cylinders becomes essentially equivalent to the corresponding behaviour of a series of rings, which are joined together but vibrate independently.

The validity of this latter argument is further justified from the results shown in Figure 3. There, for three different stiffness ratios ( $E_1/E_2 = 2, 5$  and  $40$ ) and for both CST and the PAR<sub>cs</sub> models, the variation of the relative difference,

$$\hat{\omega} = \frac{\omega_{I_x/R} - \omega_{L_x/R=0.25}}{\omega_{L_x/R}} \times 100, \quad (18)$$

has been drawn as a function of the ratio  $L_x/R$  ( $h/R = 0.2$ ). For highly reinforced cylinders ( $E_1/E_2 = 40$ ), both curves, and especially the one associated to the CST results, essentially coincide with the horizontal abscissa of the figure. Upon decreasing however the value of the stiffness ratio, the influence of the in-plane



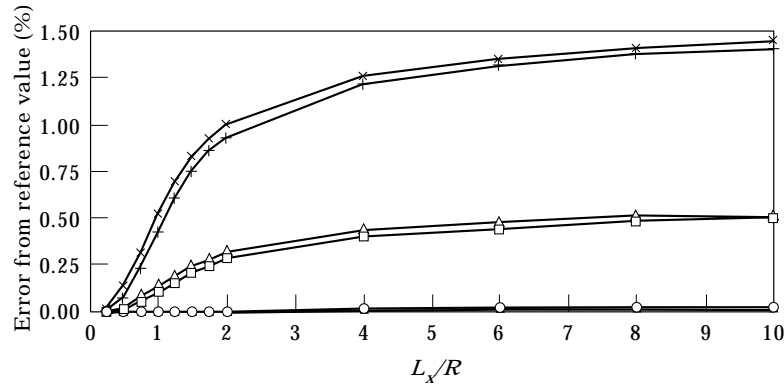


Figure 3. Relative difference [ $\hat{\omega} = ((\omega_{L_x/R} - \omega_{L_x/R=0.25})/\omega_{L_x/R}) \times 100$ ] as a function of  $L_x/R$  ( $E_1/E_2 = 2, 5, 40$ ).  $\triangle$ , CST (40);  $\circ$ , PAR<sub>cs</sub> (40);  $\diamond$ , CST (5);  $\square$ , PAR<sub>cs</sub> (5);  $\times$ , CST (2);  $+$ , PAR<sub>cs</sub> (2).

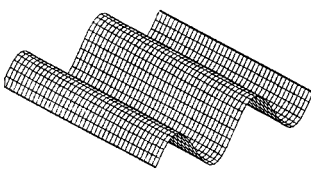
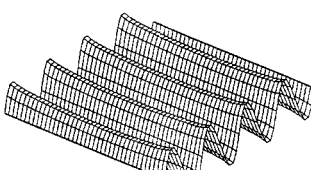
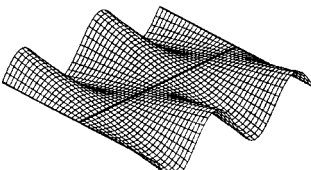
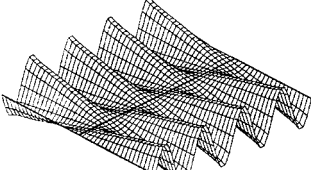
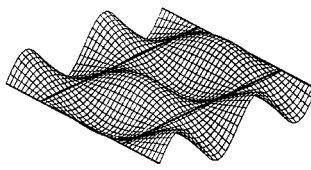
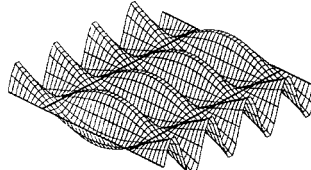
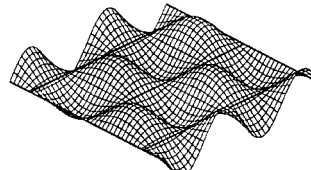
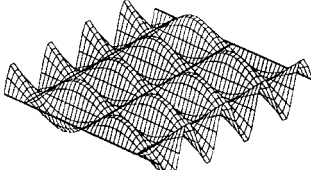
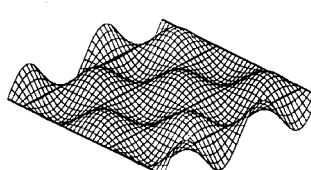
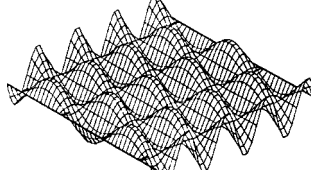
shear deformation effects increases, thus causing the gradual lift of both curves.

Dealing finally with certain homogeneous orthotropic FF cylinders, Table 6 compares the lowest frequencies obtained experimentally [26] with corresponding frequencies obtained when the present approach is applied on the PAR<sub>cs</sub> model. To the authors' best knowledge, the experimental results presented in reference [26] are the only experimental dynamic results available in the literature of FF composite cylinders. The geometrical and the material characteristics of the orthotropic cylindrical specimen considered are given in the heading of Table 6. It should be noted that these material characteristics were evaluated by a trial and error process [26], which was based on a finite element code and a plate manufactured from the same material with the cylindrical specimen. Moreover, despite certain difficulties that were experienced during the manufacturing process, a reasonably good agreement between corresponding frequencies obtained experimentally and analytically has been observed and shown in Table 6. The fact that two values of  $M$  (8 and 10) have been used for the analytical results tabulated in Table 6 shows also the degree of convergence achieved. For each one of the analytically obtained lowest frequencies, Table 6 finally shows a mapping, into the square domain  $[0, 1] \times [0, 1]$ , of the transverse component,  $w$ , of the corresponding mode shape that acts on the middle-surface ( $z = 0$ ). This makes easier the distinction of the nodal rings, which are marked with bold lines.

The simplicity of the approach and equations presented in the preceding section enables one to get accurate numerical results for different boundary conditions by just changing the orthonormal polynomial basis. This is shown in Table 7 where, in a last numerical example, the fundamental frequency parameters of a complete cantilevered cylindrical shell are presented and compared with corresponding results obtained on the basis of the state space concept [5]. The CF cylindrical shell considered is a  $[0^\circ/90^\circ/0^\circ]$  cross-ply laminated one having essentially the same geometrical and material characteristics as the FF shell employed for the corresponding results tabulated in Table 5. Here, however, the orthonormal polynomial basis (14) has been used, instead of the polynomial basis

TABLE 6

Corresponding experimental [26] and analytical fundamental frequencies  $\omega$  (Hz) for a FF homogeneous orthotropic cylindrical specimen (Data [26]:  $[0^\circ]$  lay-up,  $E_1 = 27.807$  GPa,  $E_2 = 9.887$  GPa,  $G_{12} = 3.246$  GPa,  $G_{13} = 2.533$  GPa,  $G_{23} = 2.426$  GPa,  $\nu_{12} = 0.273$ ,  $\rho = 1681.3$  kg/m<sup>3</sup>,  $L_x = 350.5$  mm,  $R = 59.18$  mm,  $h = 6.4$  mm)

Nodal rings (m)	Source of data	Circumferential half waves ( $n$ ) and normal mode shapes			
		4	Modes	8	Modes
0	Exp.	547.73		2870	
	8 pol.	546.40		2866.7	
	10 pol.	546.32		2866.4	
1	Exp.	569.32		2930	
	8 pol.	579.77		2902.7	
	10 pol.	579.60		2902.2	
2	Exp.	1400		3090	
	8 pol.	1369.2		3063.5	
	10 pol.	1368.7		3062.5	
3	Exp.	2490		3450	
	8 pol.	2353.9		3409.2	
	10 pol.	2353.0		3407.8	
4	Exp.	3550		4010	
	8 pol.	3446.3		4037.2	
	10 pol.	3345.7		3952.2	

(13). These results show again the very fast convergence of the Ritz method towards the exact fundamental frequencies of vibration. It should perhaps be noted that, in most cases, the present method converged to slightly lower

TABLE 7

*Fundamental frequency parameters  $\bar{\omega}$ , of a CF closed  $[0^\circ/90^\circ/0^\circ]$  circular cylindrical shell ( $h/R = 0.2$ ,  $E_1 = 40E_2$ ,  $G_{12} = G_{13} = 0.6E_2$ ,  $G_{23} = 0.5E_2$ ,  $\nu_{12} = 0.25$ ;  $n = 4$  unless given as a superscript)*

Theory	$L_x/R$	Ref. [5]	Present analysis				
			$M = 2$	4	6	8	10
CST	1	6.68 <sup>(2)</sup>	6.910 <sup>(2)</sup>	6.663 <sup>(2)</sup>	6.662 <sup>(2)</sup>	6.662 <sup>(2)</sup>	6.662 <sup>(2)</sup>
	2	10.90 <sup>(2)</sup>	12.263 <sup>(2)</sup>	10.902 <sup>(2)</sup>	10.897 <sup>(2)</sup>	10.897 <sup>(2)</sup>	10.897 <sup>(2)</sup>
PAR <sub>ds</sub>	1	4.98	5.420	4.965	4.934	4.932	4.932
	2	9.26	10.475	9.238	9.166	9.151	9.149
PAR <sub>cs</sub>	1	5.0	5.433	4.983	4.958	4.956	4.956
	2	9.28	10.484	9.250	9.182	9.169	9.168

frequencies than those obtained on the basis of the state space concept [5]. This however cannot be considered as a drawback of the present method, which has generally shown a very reliable behaviour. It should therefore be attributed to a rather unstable behaviour shown occasionally by the corresponding frequency determinant, during the straightforward application of the state space concept employed in reference [5], and the inevitable round off errors involved.

#### 4. CONCLUSIONS

This paper dealt with a study of the free vibration characteristics of transverse shear deformable cross-ply laminated circular cylindrical shells on the basis of the Ritz method. The analysis was based on the energy functional of the Love-type version of the unified shell theory presented in reference [28]. As a result several kinds of shear deformable Love-type shell theories were employed along with their classical counterpart. The theoretical formulation was given in a general form but the variational approach was finally applied in conjunction with a complete functional basis made of the appropriate admissible orthogonal polynomials. The method is capable of treating cross-ply laminated circular cylindrical shells subjected to any set of variationally consistent edge boundary conditions but, in this paper, particular emphasis was given to the free vibrations of shells having one or both of their edges free of external tractions.

The features and the efficiency of the proposed method was exhibited by comparing corresponding results with certain experimental data, as well as with the very few existing relevant analytical results obtained, elsewhere, on the basis of the state space concept. These comparisons showed a fast convergence of the method towards the exact frequency values, regardless of the shell theory employed. It was also concluded that orthonormal rather than simply orthogonal polynomial bases should be preferred, particularly when higher vibration frequencies and mode shapes are sought. Apart from the specific value of the present dynamic investigation, the analysis is further considered as a successful test

for its extension towards the study of corresponding problems in which the state space concept cannot be applied directly.

#### ACKNOWLEDGMENTS

The authors are grateful to the Italian National Research Council (CNR) for a short-term mobility grant awarded to Dr Messina. The work reported in this paper is an output of Dr Messina's four-week visit to the Department of Theoretical Mechanics, University of Nottingham, that was based on this grant.

#### REFERENCES

1. A. A. KHDEIR, J. N. REDDY and D. FREDERICK 1989 *International Journal of Engineering Sciences* **27**, 1337–1351. A study of bending, vibration and buckling of cross-ply circular cylindrical shells with various shell theories.
2. L. LIBRESCU, A. A. KHDEIR and D. FREDERICK 1989 *Acta Mechanica* **76**, 1–33. A shear deformable theory of laminated composite shallow shell-type panels and their response analysis I: Free vibration and buckling.
3. A. A. KHDEIR and J. N. REDDY 1990 *Computers and Structures* **34**, 817–826. Influence of edge conditions on the modal characteristics of cross-ply laminated shells.
4. A. NOSIER and J. N. REDDY 1992 *Journal of Sound and Vibration* **157**, 139–159. Vibration and stability analyses of cross-ply laminated circular cylindrical shells.
5. T. TIMARCI and K. P. SOLDATOS 1995 *Journal of Sound and Vibration* **187**, 609–624. Comparative dynamic studies for symmetric cross-ply circular cylindrical shells on the basis of a unified shear deformable shell theory.
6. T. TIMARCI 1995 *Ph.D. Thesis, Department of Theoretical Mechanics, University of Nottingham*. Vibrations of composite laminated cylindrical shells.
7. J. HADIAN and A. H. NAYFEH 1993 *Computers and Structures* **48**, 677–693. Free vibration and buckling of shear deformable cross-ply laminated plates using the state-space concept.
8. A. A. KHDEIR 1996 *Computers and Structures* **59**, 813–817. A remark on the state-space concept applied to bending, buckling and free vibration of composite laminates.
9. L. V. KANTOROVICH and V. I. KRYLOV 1964 *Approximate Methods of Higher Analysis*. The Netherlands: Noordhoff.
10. G. B. WARBURTON 1954 *Proceedings of the Institute of Mechanical Engineers* **168**, 371–384. The vibration of rectangular plates.
11. R. F. S. HEARMON 1959 *Journal of Applied Mechanics* **26**, 537–540. The frequency of flexural vibration of rectangular orthotropic plates with clamped or supported edges.
12. A. W. LEISSA 1973 *Journal of Sound and Vibration* **31**, 257–293. The free vibration of rectangular plates.
13. S. F. BASSILY and S. M. DICKINSON 1975 *Journal of Applied Mechanics* **42**, 858–864. On the use of beam functions for the problems of plates involving free edges.
14. S. F. BASSILY and S. M. DICKINSON 1978 *Journal of Sound and Vibration* **59**, 1–14. Buckling and vibration of in-plane loaded plates treated by a unified Ritz approach.
15. S. M. DICKINSON 1978 *Journal of Sound and Vibration* **61**, 1–8. The buckling and frequency of flexural vibration of rectangular isotropic and orthotropic plates using the Rayleigh's method.
16. R. B. BHAT 1985 *Journal of Sound and Vibration* **102**, 493–499. Natural frequencies of rectangular plates using characteristic orthogonal polynomials in Rayleigh–Ritz method.

17. S. M. DICKINSON and A. DI-BLASIO 1986 *Journal of Sound and Vibration* **108**, 51–62. On the use of orthogonal polynomials in the Rayleigh–Ritz method for the study of flexural vibration and buckling of isotropic and orthotropic rectangular plates.
18. P. S. FREDERIKSEN 1995 *Journal of Sound and Vibration* **186**, 743–759. Single-layer plate theories applied to the flexural vibration of completely free thick laminates.
19. T.-P. CHANG and M.-H. WU 1997 *Computers and Structures* **62**, 699–713. On the use of characteristic orthogonal polynomials in the free vibration analysis of rectangular anisotropic plates with mixed boundaries and concentrated masses.
20. P. CUPIAL 1997 *Journal of Sound and Vibration* **201**, 385–387. Calculation of the natural frequencies of composite plates by the Rayleigh–Ritz method with orthogonal polynomials.
21. N. F. HANNA and A. W. LEISSA 1994 *Journal of Sound and Vibration* **170**, 545–555. A higher order shear deformation theory for the free vibration of thick plates.
22. P. G. YOUNG and S. M. DICKINSON 1995 *Journal of Sound and Vibration* **181**, 203–214. Vibration of a class of shallow shells bounded by edges described by polynomials, part I: Theoretical approach and validation.
23. M. S. QATU 1996 *Journal of Sound and Vibration* **191**, 219–231. Vibration characteristics of cantilevered shallow shells with triangular and trapezoidal planforms.
24. D. J. GORMAN 1993 *Journal of Sound and Vibration* **165**, 409–420. Accurate free vibration analysis of the completely free orthotropic rectangular plate by the method of superposition.
25. F. MOUSSU and M. NIVOIT 1993 *Journal of Sound and Vibration* **165**, 149–163. Determination of elastic constants of orthotropic plates by modal analysis/method of superposition.
26. I. A. JONES, E. J. WILLIAMS and A. MESSINA 1996 *Proceedings of 2nd International Conference on Structural Dynamics Modelling, NAFEM, Cumbria* 267–279. Theoretical, experimental and finite element modelling of laminated composite shells.
27. C. S. KIM and S. M. DICKINSON 1985 *Journal of Sound and Vibration* **103**, 142–149. Improved approximate expressions for the natural frequencies of isotropic and orthotropic rectangular plates.
28. K. P. SOLDATOS and T. TIMARCI 1993 *Composite Structures* **25**, 165–171. A unified formulation of laminated composite, shear deformable, five-degrees-of-freedom cylindrical shell theories.
29. R. M. JONES 1975 *Mechanics of Composite Materials*. New York: Hemisphere.
30. W. H. PRESS, A. A. TEUKOSLSKY, W. T. VETTERLING and B. P. FLANNERY 1992 *Numerical Recipes in C*. Cambridge: University Press.
31. P. B. XAVIER, C. H. CHEW and K. H. LEE 1995 *International Journal of Solids and Structures* **32**, 2479–3497. Buckling and vibration of multilayer orthotropic composite shells using a simple higher-order layerwise theory.
32. L. LIBRESCU and W. LIN 1996 *European Journal of Mechanics, A/Solids* **15**, 1095–1120. Two models of shear deformable laminated plates and shells and their use in prediction of global response behavior.
33. K. P. SOLDATOS 1994 *Applied Mechanics Reviews* **47**, 501–516. Review of three dimensional dynamic analyses of circular cylinders and cylindrical shells.
34. A. W. LEISSA and J. SO 1995 *The Journal of the Acoustical Society of America* **98**, 2122–2135. Comparisons of vibration frequencies for rods and beams from one-dimensional and three-dimensional analyses.
35. A. W. LEISSA and J. SO 1995 *The Journal of the Acoustical Society of America* **98**, 2136–2141. Accurate vibration analysis of circular cylinders from three-dimensional analysis.
36. J. SO and A. W. LEISSA 1997 *Journal of Vibration and Acoustics* **119**, 89–95. Free vibrations of thick hollow circular cylinders from three-dimensional analysis.

37. J. Q. YE and K. P. SOLDATOS 1997 *Journal of Vibration and Acoustics* **119**, 317–323. Three-dimensional vibrations of cross-ply laminated hollow cylinders with clamped edge boundaries.

## APPENDIX A

The elements of the  $M \times M$  stiffness submatrices appearing in equation (12) are given as follows ( $i, j = 1, 2, \dots, M$ ):

$$(\mathbf{k}_{11})_{ij} = A_{11}(X_i^u)'(X_j^u)' + A_{66}\left(\frac{n\pi}{L_s}\right)^2 (X_i^u)^2 \delta_{ij},$$

$$(\mathbf{k}_{12})_{ij} = -\left(A_{12} + \frac{B_{12}}{R}\right)\frac{n\pi}{L_s} (X_i^u)'X_j^v + \left(A_{66} + \frac{B_{66}}{R}\right)\frac{n\pi}{L_s} X_i^u (X_j^v)',$$

$$(\mathbf{k}_{13})_{ij} = \left(\frac{A_{12}}{R} + B_{12}\left(\frac{n\pi}{L_s}\right)^2\right)(X_i^u)'X_j^w - B_{11}(X_i^u)'(X_j^w)'' - 2B_{66}\left(\frac{n\pi}{L_s}\right)^2 X_i^u (X_j^w)',$$

$$(\mathbf{k}_{14})_{ij} = B_{111}(X_i^u)'(X_j^{u1})' + B_{661}\left(\frac{n\pi}{L_s}\right)^2 X_i^u X_j^{u1},$$

$$(\mathbf{k}_{15})_{ij} = -B_{122}\left(\frac{n\pi}{L_s}\right)(X_i^u)'X_j^{v1} + B_{662}\left(\frac{n\pi}{L_s}\right)X_i^u (X_j^{v1})',$$

$$(\mathbf{k}_{22})_{ij} = \left(A_{22} + \frac{2B_{22}}{R} + \frac{D_{22}}{R^2}\right)\left(\frac{n\pi}{L_s}\right)^2 (X_i^v)^2 \delta_{ij} + \left(A_{66} + \frac{D_{66}}{R^2} + 2\frac{B_{66}}{R}\right)(X_i^v)'(X_j^v)',$$

$$(\mathbf{k}_{23})_{ij} = -\left(\frac{A_{22}}{R} + \frac{B_{22}}{R^2} + \left(\frac{n\pi}{L_s}\right)^2\left(B_{22} + \frac{D_{22}}{R}\right)\right)\frac{n\pi}{L_s} X_i^v X_j^w + \left(\frac{D_{12}}{R} + B_{12}\right)\frac{n\pi}{L_s} X_i^v (X_j^w)'' - \left(\frac{2D_{66}}{R} + 2B_{66}\right)\frac{n\pi}{L_s} (X_i^v)'(X_j^w)',$$

$$(\mathbf{k}_{24})_{ij} = -\left(\frac{D_{121}}{R} + B_{121}\right)\frac{n\pi}{L_s} X_i^v (X_j^{u1})' + \left(\frac{D_{661}}{R} + B_{661}\right)\frac{n\pi}{L_s} (X_i^v)'X_j^{u1},$$

$$(\mathbf{k}_{25})_{ij} = \left(\frac{D_{222}}{R} + B_{222}\right)\left(\frac{n\pi}{L_s}\right)^2 X_i^v X_j^{v1} + \left(\frac{D_{662}}{R} + B_{662}\right)(X_i^v)'(X_j^{v1})',$$

$$\begin{aligned}
(\mathbf{k}_{33})_{ij} &= \left( \frac{A_{22}}{R^2} + \frac{2B_{22}}{R} \left( \frac{n\pi}{L_s} \right)^2 + D_{22} \left( \frac{n\pi}{L_s} \right)^4 \right) (X_i^w)^2 \delta_{ij} + 4 \left( \frac{n\pi}{L_s} \right)^2 D_{66} (X_i^w)' (X_j^w) \\
&\quad + D_{11} (X_i^w)'' (X_j^w)'' - \left( D_{12} \left( \frac{n\pi}{L_s} \right)^2 + \frac{B_{12}}{R} \right) \left( X_i^w (X_j^w)'' + X_j^w (X_i^w)'' \right), \\
(\mathbf{k}_{34})_{ij} &= \left( D_{121} \left( \frac{n\pi}{L_s} \right)^2 + \frac{B_{121}}{R} \right) X_i^w (X_j^{u1})' - 2D_{661} \left( \frac{n\pi}{L_s} \right)^2 (X_i^w)' X_j^{u1} - D_{111} (X_i^w)'' (X_j^{u1})', \\
(\mathbf{k}_{35})_{ij} &= D_{122} \frac{n\pi}{L_s} (X_i^w)'' X_j^{v1} - 2D_{662} \frac{n\pi}{L_s} (X_i^w)' (X_j^{v1})' - \left( D_{222} \left( \frac{n\pi}{L_s} \right)^3 + \frac{B_{222}}{R} \frac{n\pi}{L_s} \right) X_i^w X_j^{v1}, \\
(\mathbf{k}_{44})_{ij} &= \left( D_{6611} \left( \frac{\pi n}{L_s} \right)^2 + A_{5511} \right) X_i^{u1} X_j^{u1} + D_{1111} (X_i^{u1})' (X_j^{u1})', \\
(\mathbf{k}_{45})_{ij} &= -D_{1212} \frac{n\pi}{L_s} (X_i^{u1})' X_j^{v1} + D_{6612} \frac{n\pi}{L_s} X_i^{u1} (X_j^{v1})', \\
(\mathbf{k}_{55})_{ij} &= \left( D_{2222} \left( \frac{n\pi}{L_s} \right)^2 + A_{4422} \right) X_i^{v1} X_j^{v1} + D_{6622} (X_i^{v1})' (X_j^{v1})', \tag{A1}
\end{aligned}$$

where a prime denotes ordinary differentiation with respect to  $x$ . Similarly, the elements of the  $M \times M$  inertia submatrices appearing in equation (12) are given as follows ( $i, j = 1, 2, \dots, M$ ):

$$\begin{aligned}
(\mathbf{m}_{11})_{ij} &= \rho_0 (X_i^u)^2 \delta_{ij}, \\
(\mathbf{m}_{22})_{ij} &= \left( \rho_0 + \frac{2\rho_1}{R} + \frac{\rho_2}{R^2} \right) (X_i^v)^2 \delta_{ij}, \quad (\mathbf{m}_{23})_{ij} = - \left( \rho_1 + \frac{\rho_2}{R} \right) \frac{n\pi}{L_s} X_i^v X_j^w, \\
(\mathbf{m}_{25})_{ij} &= \left( \rho_0^{(21)} + \frac{\rho_1^{(21)}}{R} \right) X_i^v X_j^{v1}, \quad (\mathbf{m}_{33})_{ij} = \left( \rho_0 + \rho_2 \left( \frac{n\pi}{L_s} \right)^2 \right) (X_i^v)^2 \delta_{ij} + \rho_2 (X_i^w)' (X_j^w)', \\
(\mathbf{m}_{34})_{ij} &= -\rho_1^{(11)} (X_i^w)' X_j^{u1}, \quad (\mathbf{m}_{35})_{ij} = -\rho_1^{(21)} \frac{n\pi}{L_s} X_i^w X_j^{v1}, \\
(\mathbf{m}_{44})_{ij} &= \rho_0^{(12)} (X_i^{u1})^2 \delta_{ij}, \quad \mathbf{m}_{55} = \rho_0^{(22)} (X_i^{v1})^2 \delta_{ij}, \tag{A2}
\end{aligned}$$

where  $\delta_{ij}$  is the Kronecker's symbol and,

$$\rho_m = \int_{-h/2}^{h/2} \rho z^m dz, \quad \rho_m^{(lp)} = \int_{-h/2}^{h/2} \rho (\Phi_l)^p z^m dz, \quad (m = 0, 1; l, p = 1, 2). \tag{A3}$$

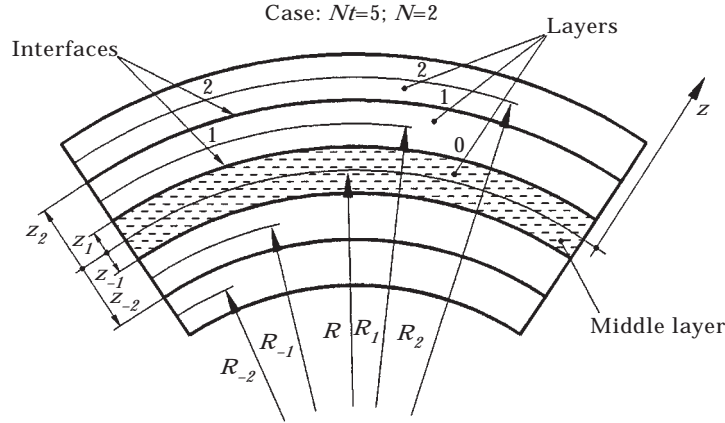


Figure 4. The nomenclature of a symmetric lay-up.

## APPENDIX B

Consider the cross-ply laminated cylindrical panel shown in Figure 4, which is composed of an odd number of coaxial layers (say  $2N + 1$ ) arranged in the form of a symmetric lay-up. Denote with a superscript 0 all quantities referring to the middle layer and denote with  $z_k$  and  $R_k$  the co-ordinate of the material interface between the  $(k - 1)$ th and the  $k$ th layer ( $k = 0, \pm 1, \pm 2, \dots, \pm N$ ) and the middle-surface radius of the  $k$ th layer, respectively. According to the analysis presented in reference [5], the following choice of global shape functions:

$$\begin{aligned}\Phi_1(z) &= A_k \varphi_1^{(k)}(z) + B_k, \\ \Phi_2(z) &= C_k \varphi_2^{(k)}(z) + (1 + z/R_k)E_k,\end{aligned}\quad (\text{A4})$$

can accommodate very accurately all interlaminar continuity and lateral surfaces boundary conditions, for any combination of local shape functions  $\varphi_1^{(k)}$  and  $\varphi_2^{(k)}$ . The exact form of the coefficients appearing in equations (A4) are as follows [5] ( $k = 0, \pm 1, \pm 2, \dots, \pm N$ ):

$$\begin{aligned}A_k &= \frac{Q_{55}^{(k \mp 1)}}{Q_{55}^{(k)}} \frac{\varphi_1'^{(k \mp 1)}(z_k)}{\varphi_1'^{(k)}(z_k)} A_{k \mp 1}, & A_0 &= 1, \\ B_k &= B_{k \mp 1} + [\varphi_1^{(k \mp 1)}(z_k)A_{k \mp 1} - \varphi_1^{(k)}(z_k)A_k], & B_0 &= 0, \\ C_k &= \frac{Q_{44}^{(k \mp 1)}}{Q_{44}^{(k)}} \frac{\varphi_2'^{(k \mp 1)}(z_k)}{\varphi_2'^{(k)}(z_k)} C_{k \mp 1}, & C_0 &= 1, \\ D_k &= \frac{1 + z_k/R_{k \mp 1}}{1 + z_k/R_k} D_{k \mp 1}, & D_0 &= 1, \\ E_k &= (D_k/D_{k \mp 1})E_{k \mp 1} + (1 + z_k/R_k)^{-1}[\varphi_2^{(k \mp 1)}(z_k)C_{k \mp 1} - \varphi_2^{(k)}(z_k)C_k], & E_0 &= 0.\end{aligned}\quad (\text{A5a-e})$$

The derivation of equations (A4) was however based on a slight approximation.



In order to eliminate this approximation in the advanced version of the parabolic shear deformable shell theory, the local shape functions employed here are defined as follows ( $k = 0, \pm 1, \pm 2, \dots, \pm N$ ):

$$\begin{aligned}\varphi_1^{(k)}(z) &= z(1 - 4z^2/3h^2), \\ \varphi_2^{(k)}(z) &= z(1 - E_k/C_k R_k) - 4z^3/3h^2.\end{aligned}\quad (\text{A6})$$

As can easily be verified, this choice of local shape functions satisfies exactly the zero shear traction boundary conditions imposed on the lateral shell surfaces, regardless of the value of the appearing constants  $C_k$ , and  $E_k$ . The remaining difficulty however is that these two constants,  $C_k$  and  $E_k$ , are now interrelated by means of equations (A5c) and (A5e). Upon inserting the second of equations (A6) into equations (A5c) and (A5e), one indeed obtains,

$$C_k = \frac{Q_{44}^{(k \mp 1)}}{Q_{44}^{(k)}} C_{k \mp 1} + \left( \frac{E_k}{R_k} - \frac{Q_{44}^{(k \mp 1)}}{Q_{44}^{(k)}} \frac{E_{k \mp 1}}{R_{k \mp 1}} \right) \frac{1}{\varphi'(z_k)}, \quad (\text{A7})$$

and

$$E_k = \left( \frac{D_k}{D_{k \mp 1}} - \frac{z_k/R_{k \mp 1}}{1 + z_k/R_k} \right) (1 + z_k/R_k) E_{k \mp 1} + (C_{k \mp 1} - C_k) \varphi(z_k), \quad (\text{A8})$$

respectively. The decoupling of  $C_k$ , and  $E_k$  is finally achieved by inserting (A7) into (A8). This yields,

$$E_k = \frac{\left[ \frac{D_k}{D_{k \mp 1}} - \frac{z_k/R_{k \mp 1}}{1 + z_k/R_k} + \frac{\varphi(z_k)}{\varphi'(z_k)} \frac{Q_{44}^{k \mp 1}}{Q_{44}^k} \frac{1}{R_{k \mp 1}} \right] E_{k \mp 1} + C_{k \mp 1} \left( 1 - \frac{Q_{44}^{k \mp 1}}{Q_{44}^k} \right) \varphi(z_k)}{1 + \frac{\varphi(z_k)}{\varphi'(z_k)} \frac{1}{R_k}}, \quad (\text{A9})$$

where,

$$\varphi(z_k) = z_k(1 - 4z_k^2/3h^2), \quad \varphi'(z_k) = 1 - 4z_k^2/h^2. \quad (\text{A10})$$

Hence, the global shape functions employed in the present advanced version of the parabolic shear deformable shell theory were still obtained on the basis of equations (A4) and (A5), in which however the definitions of the coefficients  $C_k$  and  $E_k$  given by equations (A5) were replaced in accordance with equations (A7) and (A9). These replacements guarantee for the through-thickness, continuous, parabolic distributions of the transverse shear stresses as well as for their exact nullification on the lateral shell surfaces.